Progress in Medical Devices
ISSN: 2957-5478

Zentime

Research Article https://doi.org/10.61189/883654uegazz

Optimization design and performance study of magnesium alloy vascular clamp

Weiwei Fan, Lin Mao, Bojun Liu, Chengli Song

Shanghai Institute for Minimally Invasive Therapy, School of Health Science and Engineering, University of Shanghai for Science and Technology, 200093, China.

Corresponding author: Lin Mao.

Declaration of conflict of interest: None.

Received March 21, 2024; Accepted June 5, 2024; Published September 30, 2024

Highlights

- A V-shaped vascular clamp featuring a locking mechanism and transverse teeth has been developed.
- Comparative analysis of clamps with various inner diameters reveals optimal closure with specific configurations.
- The designed clamp presents superior stress-strain response, robust clamping force, and consistent corrosion resistance.

Abstract

Purpose: This study investigates the effects of varying inner diameter of a vascular clamp made from an Mg–Nd–Zn–Zr alloy on its functional performance. The primary objectives are to optimize the clamp's structure, assess its performance across different inner diameters, and ultimately determine the optimal configuration. **Methods**: We developed a V-shaped vascular clamp equipped with a locking mechanism and transverse teeth. The study involved comparing vascular clamps with various inner diameters (0.35 mm, 0.4 mm, 0.5 mm and 0.6 mm, denoted as R0.35, R0.4, R0.5 and R0.6, respectively), achieved by modifying the clamp design. Finite element analysis simulated the closure process of these clamps, both with and without blood vessels, to analyze stress and strain distribution. Subsequently, we manufactured a clamp with the optimized design and conducted performance evaluations, including a closing strength test and an in vitro immersion test. **Results**: Among the tested vascular clamps, the R0.5 clamp demonstrated the lowest strain (0.50798) and minimal stress on blood vessels (0.7629 MPa). Notably, the R0.5 clamp remained intact during clamping fracture experiments and demonstrated a maximum closing force of 334.98±15.4 mmHg. Regarding corrosion resistance, the clamped position showed a higher corrosion rate (0.179±0.00551 $mg.cm^{-2}.day^{-1}$) compared to the open clamp (0.161±0.00306 $mg.cm^{-2}.day^{-1}$). **Conclusion**: The R0.5 clamp demonstrated superior performance in finite element analysis, showing effective vascular closure, strong clamping force, and uniform corrosion behavior. Overall, these results highlight its potential as an effective tool for vascular closure.

Keywords: Degradable magnesium alloy, hemostatic clip laparoscopic, surgery structural design, finite element analysis, corrosion behavior

Introduction

The vascular clamp, a pivotal advancement in medical technology, plays an essential role in surgical clamping and closing blood vessels, and it can also serve as a tool for secure attachment [1]. Currently, pure titanium (T) or titanium alloy vascular clips are extensively used in abdominal surgery, favored for their high strength, excellent ductility, and biocompatibility, which ensure secure and complete vascular occlusion. However, the use of titanium alloy clips can present certain drawbacks.

A significant drawback of titanium alloys is their slow degradation rate in the human body, leading to permanent implantation. This can potentially cause long-term allergic reactions [2, 3]. Moreover, the X-ray absorption coefficient of

Address correspondence to: Lin Mao, School of Health Science and Engineering, University of Shanghai for Science and Technology, No.516 Jungong Road, Yangpu District, Shanghai 200093, China. Tel: +86-21-55572159. E-mail: linmao@usst.edu.cn.

titanium alloys is substantially higher than that of human tissues, posing risks of interference with imaging exams and possible misdiagnoses. Postoperative complications associated with titanium clips include loosening, displacement, and premature detachment. These problems can lead to medical complications such as biliary leakage or bleeding, requiring a second surgery for clip removal [3].

In response to these challenges, the development of biodegradable Lapro-Clips, made from polymers, represents a significant innovation. These clips naturally degrade and are absorbed by the body after fulfilling their hemostatic role, thereby eliminating the risks associated with permanent clips. However, these polymer clips have a significantly lower strength compared to metal clips. To compensate for their reduced elastic modulus and strength while enhancing clamping force, the size of Lapro-Clips needs to be increased [4]. Additionally, the complexity of their structure can hinder their widespread application and implantation in the human body.

Magnesium and its alloys increasingly employed as biomedical metals in medical devices such as bone nails, cardiovascular stents, anastomosis nails, and vascular clamps. Magnesium alloys are also renowned as revolutionary metallic implant materials [5, 6]. Vascular clamps made from magnesium and its alloys provide promising biodegradability, biocompatibility, mechanical compatibility, and safe and reliable clamping performance, making them a low-cost and easy-to-use option, potentially eliminating the need for secondary operations [7].

Compared to traditional vascular clamp materials, magnesium alloy stands out with its lower density, higher specific strength and stiffness, and an elastic modulus similar to human bone [8-11]. However, due to the low corrosion resistance of magnesium alloys, apical cracks and excessive corrosion often occur during the use, resulting in poor sealing effects [12]. Additionally, the poor malleability of magnesium alloy makes them prone to deformation and excessive stress and strain, resulting in the rupture of the vascular clamp [13, 14].

To overcome these drawbacks, ongoing research efforts aim to refine the properties of magnesium alloy through innovative structural designs and advanced processing techniques. For example, Ikeo N et al. recently developed a Mg-Zn-Ca vascular clamp with improved ductility via casting, extrusion, blanking, and heat treatments [15]. Additionally, Ding et al. designed a circular, “V” shaped clamp using Mg-2Zn-0.2Ca and Mg-4Zn-0.2Ca materials, specifically preventing fracture during the clamping process [4].

Magnesium alloys are at the forefront of research as promising implant materials, with various alloys like AZ91, AZ31, WE43, WE54, and the biodegradable Mg-Nd-Zn-Zr being extensively studied [16]. Commercial magnesium alloys like AZ31 and WE43 were primarily designed for structural applications, emphasizing mechanical properties such as strength and toughness. However, when used as degradable biomaterials, they exhibit notable limitations. Furthermore, most AZ series magnesium alloys contain aluminum (Al), which, in physiological conditions, can act as a neurotoxin, potentially leading to Alzheimer's disease or muscle fiber damage [17, 18].

In physiological environments, the main issue with magnesium and magnesium alloys is their poor corrosion resistance, which may result in insufficient mechanical performance of implants during tissue healing, hindering their clinical application [19]. In contrast, Mg-Nd-Zn-Zr alloy (abbr. JDBM), designed specifically as a degradable biomaterial, offers better corrosion resistance and superior mechanical properties and biocompatibility compared to commercial alloys [20].

This research builds on prior studies, employing finite element analysis to optimize the clamp’s structure for effective blood vessel occlusion. Subsequently, we employed a laser cutting process to fabricate the clamp according to the optimized design. We performed tests to measure the clamping force and assess the likelihood of clamp rupture. Additionally, we conducted in vitro immersion tests to evaluate the corrosion behavior of the magnesium alloy vascular clamp in artificial plasma, enhancing our understanding of the corrosion process involved.

Materials and methods

Structural design and optimization

The magnesium alloy vascular clamp studied here was meticulously represented using SolidWorks, as shown in **Figures 1A-B**, highlighting a 0.4 mm radius. **Figure 1C** displays the clamp’s structural dimensions, while **Figure 1D** shows the tooth profile

Table 1. Size parameters of transverse tooth parameter

Transverse tooth parameter	Tooth length		Tooth height	Tooth pitch
	L1 (mm)	L2 (mm)	h (mm)	p (mm)
	0.1	0.2	0.1	0.1

Table 2. Mooney-Rivlin 5 Model Parameters

	Input parameters
Mooney-Rivlin 5 model	C10 = 1.89×10^{4} Pa
	C01 = 2.75×10^{3} Pa
	C20 = 8.572×10^{4} Pa
	C11 = 5.9043×10^{5} Pa
	C02 = 0 Pa
	Incompressible parameters D1 = 5×10^{-5} Pa^{-1}

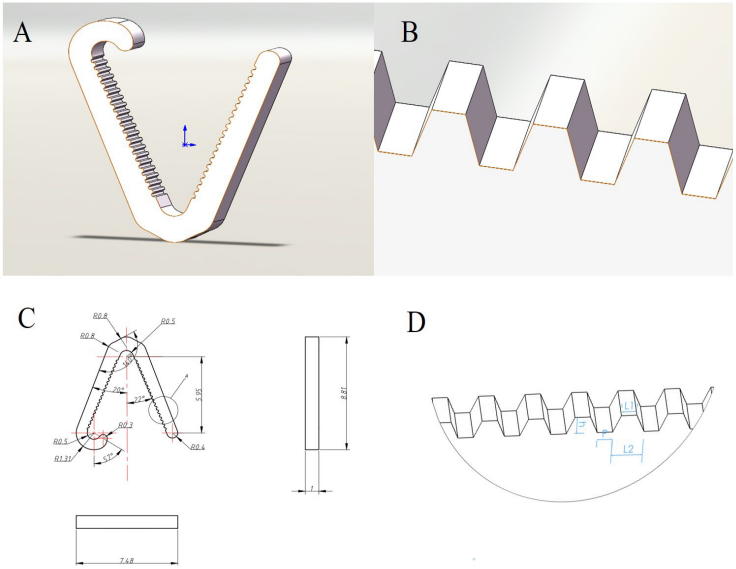

Figure 1. Modeling and structural dimensions of the designed vascular clamp. (A) Geometric model of the vascular clamp; (B) Lateral tooth details of the vascular clamp; (C) Schematic diagram of vascular clamp and structure size; (D) Transverse tooth structure dimension diagram.

parameters: L2 is the lower tooth length and L1 is the upper tooth length (L2=2L1); h is the tooth height; and p is the tooth pitch. Detailed parameters are provided in **Table 1.**

The clamp wall is intentionally designed with a gradually increasing thickness from the end to the top, effectively preventing breakage at the top during clamp usage. The top of the clamp is rounded and features a smaller opening, making it easier for the clamp to snugly fit against the blood vessel wall and clamp the vessel. To enhance friction between the clamp and the blood vessel wall and minimize clamp slippage, small transverse teeth are incorporated within the clamp design [21]. Additionally, a locking structure is introduced at the upper end of the left arm of the vascular clamp, improving its closure performance and preventing potential shifting or detachment during later stages of use.

Finite element simulation analysis

During blood vessel clamping, the mechanical properties of the vascular clamp undergo changes. We employed the finite element analysis software ANSYS Workbench to assess the stress and strain experienced by the vascular clamp under two conditions: non-blood vessel closure and blood vessel closure. Vascular clamps were fabricated using Mg-Nd-Zn-Zr alloy. The chosen intermediate venous segment had an internal diameter of 2.5 mm, a wall thickness of 0.25 mm, and a length of 10 mm. The blood vessel material was modeled using the Mooney-Rivlin 5 model with rubber-like properties. The parameters of this model are detailed in **Table 2**.

In the simulation, the assembly model of the magnesium alloy clamp and the blood vessel was imported into ANSYS Workbench 19.2 for finite element analysis and mesh generation.

Both blood vessel closure and non-blood vessel closure simulation processes employed hexahedral grids, with grid refinement applied to regions prone to stress concentration. The presence of transverse teeth led to non-uniform and relatively sparse grid generation on the transverse tooth cross-sections, necessitating grid refinement on these two lateral surfaces to achieve grid uniformity. The sweep method was utilized for further optimization of the vascular clamp grid, with the outer cross-sections serving as source faces and the entire vascular clamp as the target face. To ensure convergence of the calculation for closing the vascular clamp around the vessel, further grid refinement of the vessel is necessary. The transverse sections on both sides of the vessel

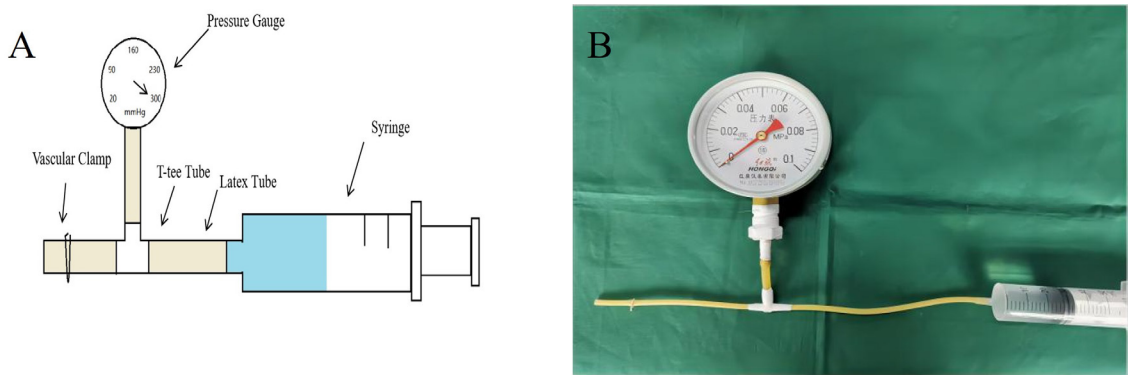

Figure 2. Test device for mechanical properties. (A) Theoretical diagram of mechanical properties test device; (B) Actual mechanical properties test device. Figure 2B is from the Research Center for Shanghai Institute for Minimally Invasive Therapy, School of Health Science and Engineering, University of Shanghai for Science and Technology.

Table 3. Simulated body fluids (artificial plasma) parameters

	Reagent name	Capacity(g/L)
Simulated body fluids (artificial plasma)	NaCl	6.8
	$NaHCO_3$	2.2
	KCl	0.4
	Na_2HPO_4	0.126
	$CaCl_2$	0.2
	$MgSO_4$	0.1
	NaH_2PO_4	0.026

are selected for Face Meshing, which generated mapped grids. The internal grid layers of the selected faces were adjusted to refine the grid count of the vessel. Meanwhile, mapped grids, known for their precision, facilitate faster solution speeds compared to free grids.

In finite element analysis, appropriate boundary conditions were established to reflect the real-world behavior of the vascular clamp during the vessel clamping process. The model's boundary conditions included applying opposite and moving displacements to the two arms of the clamp and securing the outer arc surface with Fixed Support to prevent shifting. To handle simulated deformation and hyperelastic material incorporation, the Large Deflection switch was activated. Additionally, the Analysis Settings were adjusted to include an automatic load step with additional manual load steps configured. To simulate blood vessel closure, the cross-section of one side was stabilized with Fix Support, and Nonlinear Adaptive Region was used to address convergence difficulties caused by blood vessel mesh deformation.

Closing strength property

To simulate and test the mechanical properties of the vascular clamp in vitro, we utilized a testing device as illustrated in **Figure 2A**. This device consists of a pressure gauge, a latex tube with an inner diameter of 2 mm and an outer diameter of 4 mm, a T-tee tube, and a syringe. The images of the mechanical property testing device are depicted in **Figure 2B**. Here, the latex tube serves as a blood vessel substitute. The T-tee tube facilitates the connection between the pressure gauge and the latex tube. One side of the latex tube is clamped using the clamp to simulate the closure of the blood vessel, while the other side is connected to a syringe containing simulated body fluid. Details of the simulated body fluid are provided in **Table 3**.

The procedure begins by securing the left side of the latex tube with the vascular clamp. Next, simulated body fluid was then gradually injected into the tube via the syringe. As the clamp fails to fully occlude the latex tube, the pressure gauge needle will move, indicating leakage from the rubber tube. The maximum pressure noted on the gauge at this point was recorded. Finally, the experiment was repeated thrice to calculate the average maximum closing force exerted by the vascular clamp.

In vitro corrosion performance

The corrosion behavior and degradation patterns of the magnesium alloy vascular clamp were meticulously examined through an in vitro immersion test using artificial plasma, with parameters outlined in **Table 3**. Both open-

Table 4. Comparison of tip deformation, maximum equivalent plastic strain and maximum stress of vascular clamp with different inner diameters

	Vascular clamp diameter		
	R0.35	R0.4	R0.5
Tip deformation (mm)	3.2398	3.2354	3.0889
Maximum equivalent plastic strain	0.51065	0.56558	0.49335
Maximum equivalent stress (MPa)	221.05	221.65	213.5

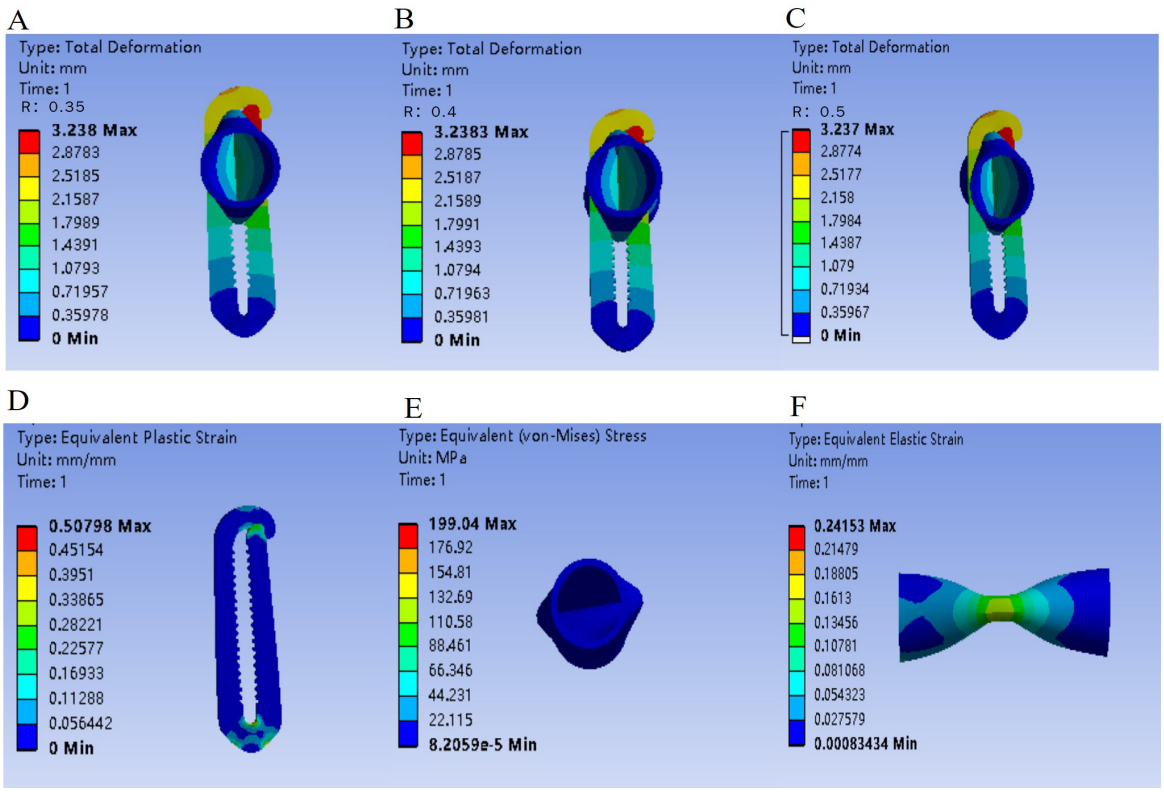

Figure 3. Mechanical simulation cloud image of vascular clamp (R0.35, R0.4, R0.5). (A-C) Deformation cloud images of the clamps (R0.35, R0.4, R0.5); (D) Equivalent plastic strain distribution of R0.5 clamp after vascular closure; (E) Diagram of stress distribution of blood vessels clamped by R0.5 clamp; (F) Strain distribution of blood vessels clamped by R0.5 clamp.

clamp and closed-latex tube clamps were tested simultaneously.

The immersion test followed the ASTM-G31-72 standard. The ratio of artificial plasma volume (ml) to the vascular clamp surface area (cm^2) was 1.8 ml/mm^2. The solution was maintained in a thermostatic water bath at 37±0.5 °C and changed every 24 hours to simulate a dynamic physiological environment. After soaking for 24 hours, the hydrogen gas produced from the degradation of the magnesium alloy vascular clamp was measured using an inverted scale pipette.

The pH value of the solution after 24 hours of immersion was measured using a pH meter. After the designated period, the sample was removed, rinsed, dried, and cleaned with a standard chromic acid solution. The clamps were then weighed. The difference in weight before and after immersion represents the weight loss.

Three sets of parallel samples were taken for each group. The corrosion rate (CR) of the magnesium alloy vascular clamp in artificial plasma was calculated using the formula:

$$CR = (8.76 \times 104 \times W) / (A \times T \times D)$$

Where:

W (g) is the weight change of the clamp.

A (cm^2) is the surface area of the clamp.

T (hours) is the immersion time.

D (g/cm^3) is the density of the magnesium alloy.

Results

Mechanical simulation results and analysis

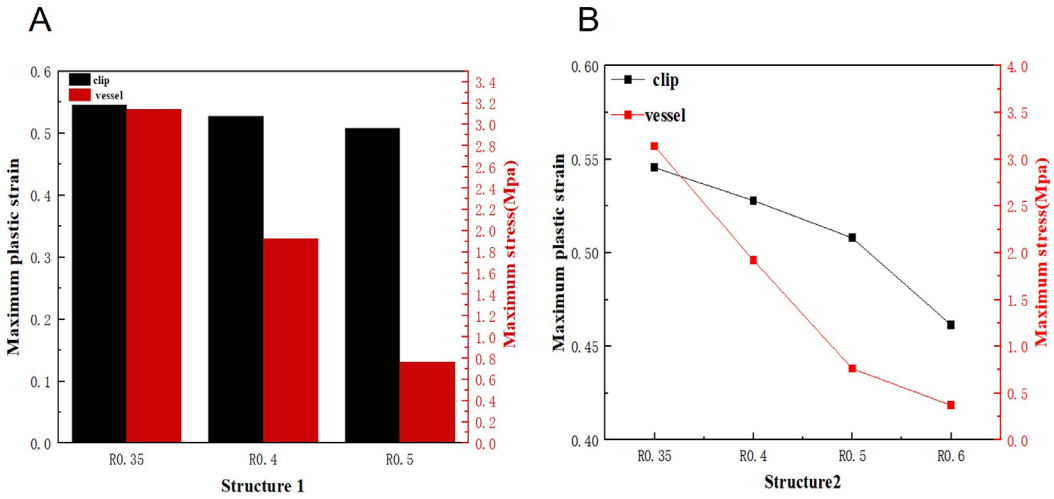

Figure 4. The maximum equivalent plastic strain and the maximum equivalent stress of blood vessel with different inner diameter clamp. (A) the finite element analysis results of three types of vascular clamps (R0.35, R0.4, and R0.5); (B) the decreasing trends of maximum strain and stress in vessels with different clamp diameters (R0.35, R0.4, R0.5, R0.6).

This section presents the results of finite element simulation aimed at elucidating the impact of various inner diameters on vascular occlusion in the absence of blood vessels. As detailed in **Table 4**, a key finding is the inverse relationship between the inner diameter of the vascular clamp and the maximum equivalent plastic strain. Specifically, the strain reached its lowest, 0.49335, at an inner diameter of 0.5 mm, indicating the most favorable outcome among the tested diameters.

Among the three inner diameters, the R0.4 vascular clamp exhibited the highest maximum equivalent stress at 221.65 MPa. Conversely, the R0.5 vascular clamp demonstrated a slightly lower maximum stress of 213.5 MPa, representing a 3.68% reduction compared to the R0.4 vascular clamp. The differences in tip deformation across the three vascular clamps were relatively minor, yet the R0.35 clamp exhibitsed more deformation, whereas the R0.5 clamp showed the least.

Based on these results, it can be concluded that the R0.5 scheme is optimal for minimizing tip deformation, achieving the lowest maximum plastic strain, and generating the smallest maximum equivalent stress.

Figures 3A-C illustrate the deformation cloud images of the vascular clamps for blood vessels with different inner diameters (R0.35, R0.4, R0.5). Notably, the tip deformation across all three clamp sizes was consistent, approximately 3.2 mm. These images clearly demonstrate the clamps' effective closure mechanism, highlighting their ability to completely occlude blood vessels without leaving any gaps, thus meeting surgical requirements.

Figure 3D displays the distribution of equivalent plastic strain in the R0.5 vascular clamp after vessel closure. The maximum plastic strain occurred at the inner arc of the top section of the clamp, aligning with the area of the highest stress concentration. Examining the stress distribution cloud diagram in **Figure 3E**, the maximum stress recorded is 199.04 MPa. **Figure 3F** presents the strain cloud diagram of a blood vessel closed by the R0.5 clamp, showcasing the maximum strain of 0.24153 experienced by the blood vessel. Despite the inevitable local stress concentration after the vessel clamping, a well-designed structure can minimize stress within the blood vessels, achieving the smallest maximum plastic strain of the vascular clamp and reducing the maximum equivalent stress on the particular blood vessel segment.

Figure 4A presents the finite element analysis results of three types of vascular clamps: R0.35, R0.4, and R0.5. The maximum equivalent plastic strain was 0.54551 for the R0.4 clamp, 0.5279 for the R0.35 clamp, and 0.50798 for the R0.5 clamp, with R0.5 clamp exhibiting the lowest strain. As the inner diameter of the vascular clamp increases, the maximum strain gradually decreases. The maximum stress was 3.1388 MPa for the R0.35 clamp, 1.9215 MPa for the R0.4 clamp, and 0.7629 MPa for the R0.5 clamp, representing a 75.7% decrease from the R0.35 clamp and a 54.9% decrease from the R0.4 clamp, indicating superior performance.

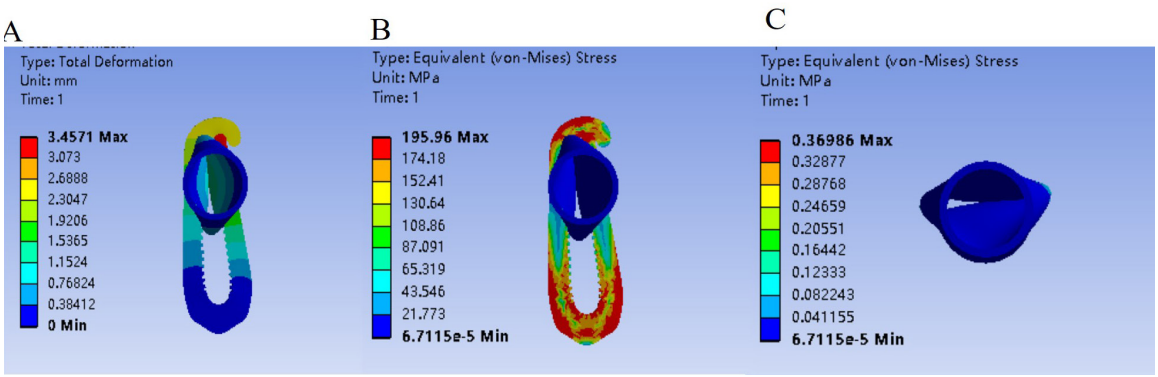

Figure 5. Mechanical simulation cloud image of R0.6 vascular clamp. (A) Deformation cloud image of the R0.6 clamp; (B) Stress distribution cloud map of the clamp; (C) Stress distribution diagram of blood vessels clamped by R0.6.

Table 5. Maximum closing force of magnesium alloy vascular clamp.

	R0.5 magnesium alloy vascular clamp
Sample 1	43 kPa
Sample 2	46 kPa
Sample 3	45 kPa
Mean pressure (kPa)/ (mmHg)	44.66±2.05 kPa / 334.98±15.4 mmHg

Figure 4B illustrates the decreasing trends of maximum strain and stress in vessels with increased clamp diameters. However, subsequent analysis with the inclusion of the R0.6 clamp closure reveals that although it further reduces stress and strain, it fails to meet the requirements for vessel closure performance due to its inability to fully close the vessels.

The finite element simulation results clearly demonstrate the superior performance of the R0.5 vascular clamp over its counterparts with smaller inner diameters. To rigorously assess the structural efficacy of the R0.5 clamp, the study introduces the R0.6 vascular clamp, featuring an increased internal diameter. Vascular clamping simulations were conducted using blood vessels, and the outcomes are presented in **Figure 5**.

The results indicate that, despite the smaller strain after blood vessel closure (0.46138) and lower stress on blood vessels (0.36986 MPa) exhibited by the R0.6 clamp compared to the R0.5 clamp (strain: 0.50798, stress: 0.7629 MPa), there are noticeable shortcomings. The tip deformation of the R0.6 clamp (3.4571) exceeded that of the R0.5 clamp (3.237). Moreover, during the vascular clamping simulation, it was observed that there were significant gaps between the two arms of the clamp, resulting in incomplete closure of the blood vessels. This phenomenon hinders effective hemostasis and may lead to postoperative bleeding, ultimately compromising the success of the procedure. Consequently, the structural optimality of the R0.5 clamp is re-affirmed.

Test result of closure strength

The experimental results on closure strength are presented in **Table 5**. The average pressure of the R0.5 magnesium alloy vascular clamp was measured to be 44.66±2.05 kPa, corresponding to 334.98±15.4 mmHg. Normal systolic blood pressure in humans ranges from 90-140 mmHg, while individuals with grade III hypertension typically have a systolic blood pressure of around 180 mmHg (24 kPa), which is considerably lower than the pressure gauge reading of 300 mmHg. Therefore, it can be inferred that the maximum average pressure value (334.98±15.4 mmHg) measured by the experiment for the vascular clamp during actual closure exceeds the normal blood pressure range for humans and even surpasses the systolic blood pressure of hypertensive individuals, indicating a notable capacity to tolerate high pressures.

In vitro corrosion performance

The corrosion characteristics of Mg-Nd-Zn-Zr vascular clamps were investigated through in vitro immersion tests, assessing both hydrogen evolution and pH value measurements. **Figure 6A** illustrates the daily hydrogen evolution volume of Mg-Nd-Zn-Zr vascular clamps immersed in artificial plasma, indicating a volume below 0.3 ml/cm^2. Over the 10-day

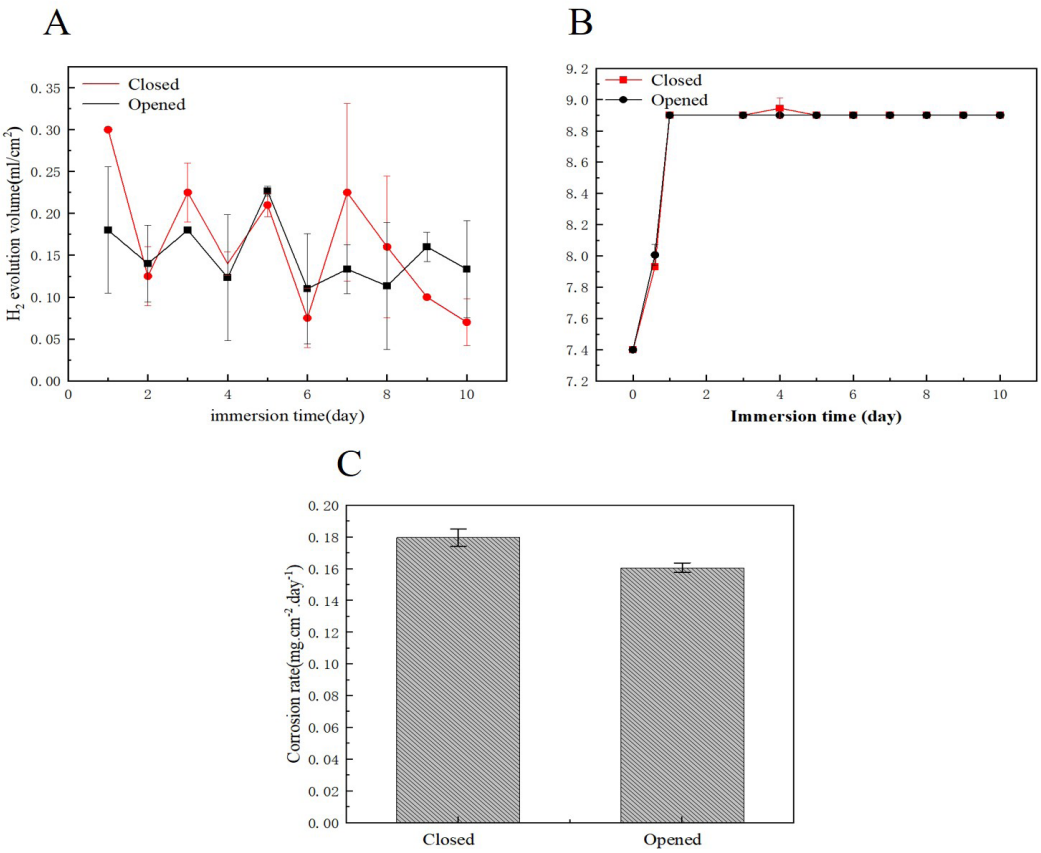

Figure 6. Results of in vitro immersion tests for magnesium alloy vascular clamp. (A) Daily hydrogen evolution of R0.5 vascular clamp in artificial plasma solution; (B) PH value of artificial plasma for the immersion of R0.5 magnesium alloy vascular clamp; (C) Corrosion rate of magnesium alloy vascular clamp.

experimental period, the closed clamp exhibited a higher average hydrogen evolution sum (1.63±0.1539 ml/cm^2) compared to the open clamp (1.58±0.1334 ml/cm^2), as demonstrated by experimental data analysis.

Figure 6B depicts the pH dynamics of the artificial plasma over the immersion time for the Mg-Nd-Zn-Zr vascular clamp. It is evident from **Figure 6C** that within the initial 24 hours of immersion, the pH value of the of the immersion medium for Mg-Nd-Zn-Zr vascular clamp increased rapidly from 7.4 to approximately 8.9. Subsequently, the pH changes gradually leveled off, stabilizing around 8.9 after the second day of immersion.

The corrosion rate of the Mg-Nd-Zn-Zr vascular clamp was determined using weight loss experiments, and the corresponding bar graph is displayed in **Figure 6C**. The average corrosion rate for the closed magnesium alloy vascular clamp was calculated as 0.179±0.00551 mg·cm^{-2}·day^{-1}, while the average corrosion rate for the open magnesium alloy vascular clamp was 0.161±0.00306 mg·cm^{-2}·day^{-1}. These results align with the corrosion rate derived from weight loss, indicating a higher corrosion rate for the closed vascular clamp compared to the open vascular clamp in the artificial plasma solution.

Discussion

Laparoscopic surgery often encounters challenges related to bleeding and the need for timely hemostasis. The development of the vascular clamp represents a significant advancement in medical hemostatic tools. Traditional hemostatic tools, such as surgical sutures and anastomosis nails, have their limitations. Sutures may not always provide reliable hemostasis or secure closure [22]. Anastomosis nails, on the other hand, often require multiple nails, which may increase the risk of blood leakage [23]. In comparison, the vascular clamp is smaller and more flexible, making it particularly advantageous for application in narrow tissue depths and areas that are challenging to access with standard hemostatic clamps. The vascular clamp offers improved maneuverability and precision in achieving effective hemostasis during laparoscopic surgery.

Previous studies on magnesium alloy vascular clamps primarily focused on the material's biodegradability and biocompatibility, while our design also emphasizes its mechanical reliability and ease of use [24]. The introduction of a locking mechanism to the upper end of the clamp's left arm is an essential improvement, addressing the issue of clamp displacement and detachment that was prevalent in earlier designs [25]. This feature ensures a more secure and stable closure, reducing the risk of post-surgical complications.

In laparoscopic surgery, the circular inner diameter opening at the top of the vascular clamp is pivotal in successfully closing blood vessels. The optimal size of this opening is crucial as it ensures a snug fit against the vessel wall, thereby facilitating a successful closure. However, it is also necessary to consider the structural integrity of the clamp [26].

A smaller diameter often results in a tighter curvature at the bend between the clamp's arms, leading to significant change in thickness across these components. This leads to a phenomenon called stress concentration, where the maximum stress in a localized area is much higher than the average stress the structure endures. Stress concentration can cause fracture in brittle materials and even induce fatigue cracks in ductile materials [27].

The top inner part of the vascular clamp is particularly susceptible to stress concentration due to the sudden change in shape during the clamping action. Therefore, optimizing the design of this area is a key focus of this research. We aim to find a balance between minimizing the circular inner diameter opening for efficient vessel closure and ensuring structural integrity to avoid stress concentration and potential fractures.

Based on the existing design of vascular clamp, we propose an optimized design by changing the inner diameter of the bottom side of the clamp. In addition to the existing vascular clamp of 0.4 mm, two other inner diameters were designed, 0.5 mm and 0.35 mm. The stress and strain conditions of the three inner diameters were compared to select the best structure of the vascular clamp. At the same time, the optimal performance of the vascular clamp was verified by further increasing the inner diameter of the vascular clamp.

One of the primary objectives of the vascular clamp design is to ensure complete closure of the blood vessel, thus guaranteeing its safety and stability. Through finite element simulations, our study has shown that the vascular clamp with an inner diameter of 0.5 mm exhibits the most favorable stress-strain performance during complete blood vessel closure. It has been demonstrated that clamps with larger inner diameters possess superior stress-strain characteristics during complete closure of the blood vessel. We observed that as the inner diameter increases, the stress concentration at the bend of the vascular clamp gradually diminishes, leading to a gradual reduction in stress strain. However, at an inner diameter of 0.6 mm, the contact area between the blood vessel and the clamp decreases, preventing the clamp from adequately fitting the blood vessel. Consequently, an inner diameter of 0.6 mm fails to meet the practical requirements for closing blood vessels effectively during clinical surgeries.

Conclusion

Based on the findings from two sets of simulation analyses comparing vascular clamps with varying inner diameters, the vascular clamp with an inner diameter of 0.5 mm demonstrated the most favorable mechanical properties among the three variations tested. Subsequently, an optimized Mg-Nd-Zn-Zr alloy vascular clamp was fabricated using a laser cutting method.

In the gripping force test experiment, the R0.5 vascular clamp exhibited a maximum closing force of 334.98±15.4mmHg, surpassing both the normal blood pressure value of the human body and the systolic blood pressure value of the hypertensive group (180 mmHg). This indicates that the clamp possesses strong gripping capability. Moreover, corrosion rate analysis revealed that the closed clamp (0.179 ± 0.00551 mg.cm^{-2}.day^{-1}) exhibited a slightly faster corrosion rate compared to the open clamp (0.161 ± 0.00306 mg.cm^{-2}.day^{-1}).

Consequently, the newly developed Mg-Nd-Zn-Zr alloy vascular clamp holds significant promise as an effective instrument for closing blood vessels during laparoscopic surgery.

There are several limitations to our study that should be acknowledged. Firstly, the accuracy of our results may be influenced by the assumptions and simplifications inherent in the simulation model. Moreover, the simulation analysis was conducted solely under static conditions, whereas the mechanical behavior of the vascular clamp in real-life situations is

influenced by additional factors, such as blood flow.

Further investigation into the biodegradability, a critical attribute for reducing long-term complications, are recommended. Conducting animal experiments to examine the corrosion behavior of the degradable magnesium alloy vascular clamp within the body could help simulate real surgical scenarios more accurately. Such studies would ideally include evaluations of the vascular clamp's impact through blood biochemical analysis and histological examinations, further validating its clinical applicability and safety.

Author Contributions: Lin Mao, and Weiwei Fan conceived this project. Lin Mao and Weiwei Fan carried out structural design and finite element simulation. Lin Mao and Chengli Song designed a closing strength experiment and an in vitro immersion experiment. Weiwei Fan, Bojun Liu, Xin Zheng and Yujie Zhou performed experiments and collected the relevant data and analyzed. All the authors contributed to the writing of manuscript.

References

[1] Ooi BP, Hassan MR, Kiew KK, et al. Case report of a hemostatic clip being retained for 2 years after deployment. Gastrointest Endosc 2010;72(6):1315-1316.

[2] Javed F, Al-Hezaimi K, Almas K, et al. Is titanium sensitivity associated with allergic reactions in patients with dental implants? A systematic review. Clin Implant Dent Relat Res 2013;15(1):47-52.

[3] Fage SW, Muris J, Jakobsen SS, et al. Titanium: a review on exposure, release, penetration, allergy, epidemiology, and clinical reactivity. Contact Dermatitis 2016;74(6):323-345.

[4] Ding PF, Liu YC, He XH, et al. In vitro and in vivo biocompatibility of Mg-Zn-Ca alloy operative clip. Bioact Mater 2019;4:236-244.

[5] Radha R, Sreekanth D. Insight of magnesium alloys and composites for orthopedic implant applications-a review. J Magnesium Alloys 2017;5(3):286-312.

[6] Zhao D, Witte F, Lu F, et al. Current status on clinical applications of magnesium-based orthopaedic implants: A review from clinical translational perspective. Biomaterials 2017;112:287-302.

[7] Zhang RF. Preparation and properties of biodegradable Mg-Zn-Ca alloy vascular clamp for laparoscopic surgery. Tianjin University of Technology 2017.

[8] Witte F, Kaese V, Haferkamp H, et al. In vivo corrosion of four magnesium alloys and the associated bone response. Biomaterials 2005;26(17):3557-3563.

[9] Yufeng Z, Bin L, Xuannan G. Research progress of biodegradable medical metal materials Materials Review 2009;23(1):6.

[10] Fischer J, Crostack H, Windhagen, et al. Synchrotron-radiation based microtomography for in-vivo corrosion measurements of magnesium alloys. ORS Transactions 2005.

[11] Witte F. The history of biodegradable magnesium implants: A review. Acta Biomater 2010;6(5):1680-1692.

[12] Wang RX, Hong LX, Zhang XB. Research progress in corrosion resistance of biomedical magnesium alloys. J Mater Eng 2021;49(12):14-27.

[13] Ren D, Zeng F, Liu L, et al. Bending Properties of Mg Alloy Tailored Arc-Heat-Treated Blanks. Materials 2019;12(6):977.

[14] Wang Z, Cao H, Zheng H, et al. Effect of aging treatment on the mechanical property and precipitation transformation of Mg-Co-Y alloy. Mater Sci Eng: A 2023;881:145322.

[15] Ikeo N, Nakamura R, Naka K, et al. Fabrication of a magnesium alloy with excellent ductility for biodegradable clips. Acta Biomater 2016;29:468-476.

[16] Bai H. Preparation, microstructure and in vivo and in vitro properties of magnesium alloy vascular clamp. Tianjin University of Technology 2018.

[17] Zhang Y, Li J, Li J. Effects of microstructure transformation on mechanical properties, corrosion behaviors of Mg-Zn-Mn-Ca alloys in simulated body fluid. J Mech Behav Biomed Mater 2018;80:246-257.

[18] Liu H, Zhang W, Fang Y, et al. Neurotoxicity of aluminum oxide nanoparticles and their mechanistic role in dopaminergic neuron injury involving p53-related pathways. J Hazard Mater 2020;392:122312.

[19] Abdel-Gawad SA, Shoeib MA. Corrosion studies and microstructure of Mg–Zn–Ca alloys for biomedical applications. Surf Interfaces 2019;14:108-116.

[20] Mao L, Zhou H, Chen L, et al. Enhanced biocompatibility and long-term durability in vivo of Mg-Nd-Zn-Zr alloy for vascular stent application. J Alloys Compd 2017;720:245-253.

[21] Mao L, Zheng X, Tian Y, et al. Structural Optimization, Fabrication, and Corrosion Behaviors of Biodegradable Mg-Nd-Zn-Zr Alloy Hemostatic Clip. Metals 2022;12(11):1979.

[22] Wang XC, Wu QT, Zheng ZZ, et al. Research progress of medical sutures. J Anhui Eng Univ 2020;35(05):1-11.

[23] Lei J. Preparation and research of degradable

magnesium alloy for anastomosis nail. Lanzhou University of Technology 2022.
[24] Mochizuki A, Kaneda H. Study on the blood compatibility and biodegradation properties of magnesium alloys. Mater Sci Eng C Mater Biol Appl 2015;47:204-210.
[25] Sun R, Ren LZ, Zhang ZP, et al. Pilot study of minimum occlusive force of vascular clamps on arterial vessels in rats. Sci Rep 2021;11(1):6042.
[26] Chen HY, Einstein DR, Chen K, et al. Computational Modeling of Vascular Clamping: A Step Toward Simulating Surgery. 2005 IEEE Engineering in Medicine and Biology 27th Annual Conference 2005;302-303.
[27] Wang YN, Oyen D, Guo W, et al. StressNet - Deep learning to predict stress with fracture propagation in brittle materials. npj Mater Degrad 2021;5(1):6.